IEEE Access
Multidisciplinary | Rapid Review | Open Access Journal

Received November 19, 2019, accepted December 6, 2019, date of publication December 17, 2019,
date of current version December 26, 2019.

Digital Object Identifier 10.1109/ACCESS.2019.2960399

Acceleration-Level Obstacle Avoidance of Redundant Manipulators

DONGSHENG GUO, (Member, IEEE), QINGSHAN FENG, AND JIANHUANG CAI
College of Information Science and Engineering, Huaqiao University, Xiamen 361021, China

Corresponding author: Dongsheng Guo (gdongsh@hqu.edu.cn)

This work was supported in part by the National Natural Science Foundation of China under Grant 61603143, in part by the Training Program for Outstanding Young Scientific Talents in Fujian Province University under Grant 50X19020, in part by the Quanzhou City Science and Technology Program of China under Grant 2018C111R, and in part by the Promotion Program for Young and Middle-Aged Teacher in Science and Technology Research of Huaqiao University under Grant ZQN-YX402.

ABSTRACT Avoiding obstacle during path planning is a crucial issue in redundant manipulators. In this study, the obstacle avoidance of redundant manipulators, which is investigated at acceleration level, is presented. Specifically, a new acceleration-level inequality is designed and formulated, which is proven to be capable of avoiding obstacle. By combining the end-effector planning requirement (formulated as equality constraint) and incorporating the physical limits (formulated as bound constraints), the acceleration-level obstacle avoidance (ALOA) scheme for redundant manipulators is proposed. Such scheme is transformed into a quadratic program and is computed by a numerical algorithm. Simulation results under the PA10 manipulator with different obstacles further validate the effective performance of the proposed ALOA scheme.

INDEX TERMS Acceleration-level obstacle avoidance, redundant manipulators, quadratic program.

I. INTRODUCTION

Recently, as one fundamental issue in the study of robotics, the path planning (or say, kinematic control) of redundant manipulators has attracted considerable attention and has been widely investigated [1]–[6]. In addition, during the path planning, how to make the manipulator effectively avoid environmental obstacle is a crucial issue. This is because the collision between the manipulator and obstacle would cause the failure of path planning, and may further cause the damage to the manipulator (and obstacle). Numerous studies have been reported and presented to realize the obstacle avoidance of redundant manipulators [1]–[3], [7]–[9].

One well-known obstacle-avoidance approach is based on the pseudoinverse formulation, wherein the schemes are depicted in the summation of minimum-norm and homogeneous solutions [1], [10]–[15]. For example, in [11], an obstacle-avoidance scheme with Jacobian transpose for redundant manipulators is presented. In [13], a pseudoinverse-based scheme with multi-objective achievement for avoiding obstacle is investigated. In [15], an obstacle-avoidance scheme with noise tolerance for redundant manipulators is developed. Another well-known obstacle-avoidance approach is the one aided with the artificial potential field, wherein the expected position is represented as an attractive pole and the obstacle is represented by a repulsive surface. See, e.g., [16]–[20].

Different from the aforementioned two approaches, the approach based on the quadratic program (QP) has also been studied for the obstacle avoidance of redundant manipulators [21]–[26]. For instance, Tang *et al.* [22] provided an equality for avoiding obstacle and developed the resulting QP-based scheme. Zhang and Wang [23] designed an inequality to avoid obstacle and investigated the corresponding QP-based scheme. Hu *et al.* [24] constructed another inequality for obstacle avoidance and formulated the resultant QP-based scheme. Although success has been realized using the QP-based approach [21]–[26], the existing literature mainly focuses on the study of obstacle avoidance at the level of joint velocity.

In general, the velocity-level obstacle-avoidance schemes may introduce the discontinuity issue in joint velocity [25], [27], [28]. This phenomenon is undesirable and unaccepted in practical applications. Thus, an effective acceleration-level scheme, which can prevent the discontinuity, is worth designing and investigating for the obstacle avoidance of redundant manipulators. In [27], the obstacle avoidance at acceleration level was presented for the first time. Then, the acceleration-level obstacle avoidance of redundant manipulators was further investigated in [28] and [29]. Except the three

The associate editor coordinating the review of this manuscript and approving it for publication was Guilin Yang.

works [27]–[29], nearly no research result on investigating the acceleration-level obstacle avoidance exists to date. That is, the study of acceleration-level obstacle avoidance is rare despite its importance in the path planning of redundant manipulators.

In this study, motivated by the existing literature [27]–[29], we provide and formulate another acceleration-level obstacle-avoidance (ALOA) scheme for redundant manipulators. Specifically, a new acceleration-level inequality that is proven to be capable of avoiding obstacle is designed and formulated. To the best of our knowledge, such an inequality has not been reported in the existing literature. Then, the ALOA scheme is proposed by combining the end-effector planning requirement formulated as equality constraint and incorporating the physical limits formulated as bound constraints. The proposed scheme is transformed into a QP and is computed by a numerical algorithm [27]. Under the PA10 manipulator with different obstacles, simulation results are illustrated to further validate the effective performance of the proposed ALOA scheme.

The remainder of this study is organized as follows. Section II presents the acceleration-level inequality and describes the ALOA scheme. Section III shows the QP reformulation and its solver. Section IV provides the simulation results obtained using the proposed ALOA scheme. Section V concludes this study and presents the final remarks.

II. INEQUALITY AND SCHEME FORMULATIONS

In this section, the path planning preliminary for redundant manipulators is firstly presented. Then, the acceleration-level inequality designed for avoiding obstacle is formulated. On the basis of such an inequality, the ALOA scheme for redundant manipulators is thus proposed.

A. PRELIMINARY

Mathematically, the path planning of redundant manipulators can be formulated as the online solution of the following kinematic equation [1]:

$$\varphi(\theta) = r_{\mathrm{d}}, \tag{1}$$

where $\theta \in R^n$ denotes the joint angle, $r_{\mathrm{d}} \in R^m$ denotes the end-effector desired path, and $\varphi(\cdot) : R^n \to R^m$ denotes the nonlinear mapping [1]. Simply put, given r_{d}, we need to solve for θ. With regard to a redundant manipulator, $m < n$ in (1), which means that an infinite number of θ are possible for a specified r_{d}. Moreover, because of the nonlinearity, it is generally difficult to realize the path planning by directly solving (1).

As presented in the existing literature [1]–[3], [27]–[31], the path planning of redundant manipulators can be studied at velocity level:

$$J\dot{\theta} = \dot{r}_{\mathrm{d}}, \tag{2}$$

or at acceleration level:

$$J\ddot{\theta} = \ddot{r}_{\mathrm{d}} - \dot{J}\dot{\theta}, \tag{3}$$

where $\dot{\theta}$ and $\ddot{\theta}$ denote respectively the joint velocity and joint acceleration, J denotes the manipulator Jacobian matrix [32] with $\dot{J}$ as its derivative, and $\dot{r}_{\mathrm{d}}$ denotes the derivative of r_{d} with $\ddot{r}_{\mathrm{d}}$ as its derivative. Notably, (2) and (3) are underdetermined owing to $m < n$. By solving (2) and (3) properly, the path planning with additional characteristics (e.g., repeatability and performance optimization) can be realized for redundant manipulators [30], [31].

In particular, with regard to obstacle avoidance, the schemes in [1], [10]–[15], [21]–[26] are developed on the basis of (2) (i.e., at velocity level), whereas the schemes in [27]–[29] are constructed on the basis of (3) (i.e., at acceleration level). In this study, we design a new inequality on the basis of (3) for obstacle avoidance, and propose the ALOA scheme for redundant manipulators.

B. NEW INEQUALITY FOR OBSTACLE AVOIDANCE

In general, the following two steps are required to realize the obstacle avoidance of redundant manipulators [27]–[29].

1) Calculate the distance between the manipulator's link L and obstacle point O to locate critical point C on link L.
2) Assign an additional velocity $\dot{r}_C$ or an additional acceleration $\ddot{r}_C$ at point C to make link L leave point O, thereby enabling obstacle avoidance.

The velocity-level equality and inequality that can generate additional velocity are presented in [22]–[26], while the acceleration-level inequality that can generate additional acceleration and velocity is shown in [27] and [28]. In this study, we design a new acceleration-level inequality to realize the obstacle avoidance, which is formulated as follows:

$$A\ddot{\theta} \leqslant B\dot{\theta}. \tag{4}$$

In (4), coefficient matrices A and B are obtained respectively by $A = -\overrightarrow{r}J_C$ and $B = \overrightarrow{r}\dot{J}_C$, where J_C denotes the Jacobian matrix at point C, with $\dot{J}_C$ as its derivative. Considering in the general 3-D space, the direction vector $\overrightarrow{r}$ is given by

$$\overrightarrow{r} = [x_C - x_O, y_C - y_O, z_C - z_O],$$

where (x_C, y_C, z_C) and (x_O, y_O, z_O) denote respectively the X-, Y- and Z-axis coordinates at points C and O.

With regard to the acceleration-level inequality (4), the derivation is presented in the Appendix, which indicates that (4) can generate an additional acceleration with variable magnitude and be capable of avoiding obstacle. Moreover, the procedure for generating (4) is similar to that provided in [28], and is thus omitted in this study.

There are two general methods to obtain the effective obstacle point and the corresponding critical point. One is the sensor-based method and the other is the model-based method. In this study, the latter is used, of which the detail is presented in [26]. Suppose there are ϱ pairs of obstacle and critical points. Then, $A \in R^{\varrho \times n}$ and $B \in R^{\varrho \times n}$. Furthermore, the acceleration-level inequality (4) is reformulated as follows:

$$A\ddot{\theta} \leqslant b, \tag{5}$$

where $b = B\dot{\theta} \in R^{\varrho}$. The superiority of the acceleration-level inequality (5) over the one provided in [27] and [28] is described by the following remark.

Remark 1: In the existing literature [27], [28], an acceleration-level inequality has been developed and investigated, which is formulated as $J_G\ddot{\theta} \leqslant b_G$, with $J_G \in R^{3\varrho\times n}$ and $b_G \in R^{3\varrho}$ in the 3-D space. This means that each pair of the obstacle and critical points leads to three inequalities. By contrast, each pair results in only one inequality in (5). Evidently, with a large ϱ value, the number of inequalities in $J_G\ddot{\theta} \leqslant b_G$ would be much more than that in (5). Notably, in the next section, (5) is incorporated into the scheme formulation as an inequality constraint. It is obvious that less inequalities in the formulation imply a less complex scheme. Therefore, the acceleration-level inequality (5) (and/or (4)) is advantageous over the inequality provided in [27] and [28].

C. ALOA SCHEME

Let us recall the kinematic equations at three levels, i.e., (1), (2), and (3). Considering the feedback introduction, we have the following formulation for the end-effector planning requirement at acceleration level:

$$J\ddot{\theta} = \ddot{r}_{\mathrm{d}} - \dot{J}\dot{\theta} - \alpha(J\dot{\theta} - \dot{r}_{\mathrm{d}}) - \beta(\varphi(\theta) - r_{\mathrm{d}}),$$

which is rewritten as

$$J\ddot{\theta} = d, \tag{6}$$

where $d = \ddot{r}_{\mathrm{d}} - \dot{J}\dot{\theta} - \alpha(J\dot{\theta} - \dot{r}_{\mathrm{d}}) - \beta(\varphi(\theta) - r_{\mathrm{d}})$ with $\alpha > 0 \in R$ and $\beta > 0 \in R$ being the feedback gains.

On the basis of (5) and (6), and by incorporating the physical limits, the following ALOA scheme for redundant manipulators is thus proposed in this study:

$$\begin{aligned}
&\text{minimize} && \|\ddot{\theta}\|_2^2/2 && (7)\\
&\text{subject to} && J\ddot{\theta} = d, && (8)\\
& && A\ddot{\theta} \leqslant b, && (9)\\
& && \theta^- \leqslant \theta \leqslant \theta^+, && (10)\\
& && \dot{\theta}^- \leqslant \dot{\theta} \leqslant \dot{\theta}^+, && (11)\\
& && \ddot{\theta}^- \leqslant \ddot{\theta} \leqslant \ddot{\theta}^+, && (12)
\end{aligned}$$

where symbol $\|\cdot\|_2$ denotes the two norm operator, and $\theta^{\pm}$, $\dot{\theta}^{\pm}$, and $\ddot{\theta}^{\pm}$ denote the physical limits of θ, $\dot{\theta}$, and $\ddot{\theta}$, respectively.

Remark 2: The following differences between the existing literature [27]–[29] and this study on the acceleration-level obstacle avoidance are addressed.

1) In [27] and [28], an inequality for avoiding obstacle at acceleration level is developed, and the resultant obstacle-avoidance scheme is investigated.
2) In [29], an acceleration-level performance index for avoiding obstacle is constructed, and the optimization-based obstacle avoidance scheme is discussed.
3) In this study, the new inequality (5) for avoiding obstacle is designed, which differs from the one in [27] and [28] (see also Remark 1). The resultant ALOA scheme (7)–(12) for redundant manipulators is proposed.

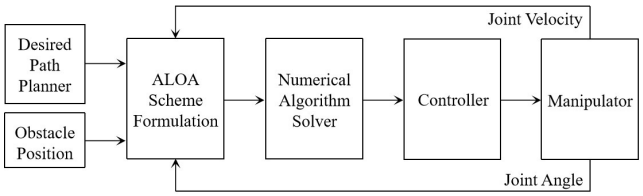

FIGURE 1. Block diagram of the acceleration-level path-planning system for redundant manipulators by combining the proposed ALOA scheme (7)–(12) and the numerical algorithm (19).

TABLE 1. Joint-physical limits utilized for the PA10 manipulator.

Joint	θ^-	θ^+	$\dot{\theta}^-$	$\dot{\theta}^+$	$\ddot{\theta}^-$	$\ddot{\theta}^+$
1	-3.3777	3.3777	-1.0	1.0	-0.3	0.3
2	-1.7639	1.7639	-1.0	1.0	-0.3	0.3
3	-3.3777	3.3777	-2.0	2.0	-0.3	0.3
4	-2.6834	2.6834	-2.0	2.0	-0.3	0.3
5	-5.0666	5.0666	-2π	2π	-0.3	0.3
6	-3.3777	3.3777	-2π	2π	-0.3	0.3
7	-6.7555	6.7555	-2π	2π	-0.3	0.3
8	-6.7555	6.7555	-2π	2π	-0.3	0.3

As demonstrated in [27]–[29] and Section IV of this study, these obstacle avoidance schemes are applicable to redundant manipulators. Thus, this study, together with [27]–[29], has presented different acceleration-level methods for realizing the obstacle avoidance. These findings provide insights into the research for the obstacle avoidance of redundant manipulators at acceleration level.

III. QP REFORMULATION AND SOLVER

This section reformulates the proposed ALOA scheme (7)–(12) as a QP that is computed by a numerical algorithm [27].

First, the bound constraints (10)–(12) are combined into one expression as follows (see [33] for details about the combination):

$$\eta^- \leqslant \ddot{\theta} \leqslant \eta^+, \tag{13}$$

with the ith elements of η^+ and η^- being given by

$$\begin{aligned}
\eta_i^+ &= \min\{\kappa_{\mathrm{p}}(\theta_i^+ - \vartheta - \theta_i), \kappa_{\mathrm{v}}(\dot{\theta}_i^+ - \dot{\theta}_i), \ddot{\theta}_i^+\},\\
\eta_i^- &= \max\{\kappa_{\mathrm{p}}(\theta_i^- + \vartheta - \theta_i), \kappa_{\mathrm{v}}(\dot{\theta}_i^- - \dot{\theta}_i), \ddot{\theta}_i^-\},
\end{aligned}$$

where $\vartheta > 0 \in R$, $\kappa_{\mathrm{p}} > 0 \in R$, and $\kappa_{\mathrm{v}} > 0 \in R$ are utilized in consideration of inertia movement [31].

Then, defining $x = \ddot{\theta}$ yields the following QP reformulation of the proposed ALOA scheme (7)–(12):

$$\begin{aligned}
&\text{minimize} && x^{\mathrm{T}}Qx/2 + p^{\mathrm{T}}x && (14)\\
&\text{subject to} && Jx = d, && (15)\\
& && Ax \leqslant b, && (16)\\
& && \eta^- \leqslant x \leqslant \eta^+, && (17)
\end{aligned}$$

where $Q = I \in R^{n\times n}$ (i.e., the identity matrix), $p = 0 \in R^n$, and superscript $^{\mathrm{T}}$ denotes the transpose operator.

Finally, according to the bridge theorems in [27], the optimal solution of the QP (14)–(17) can be determined by

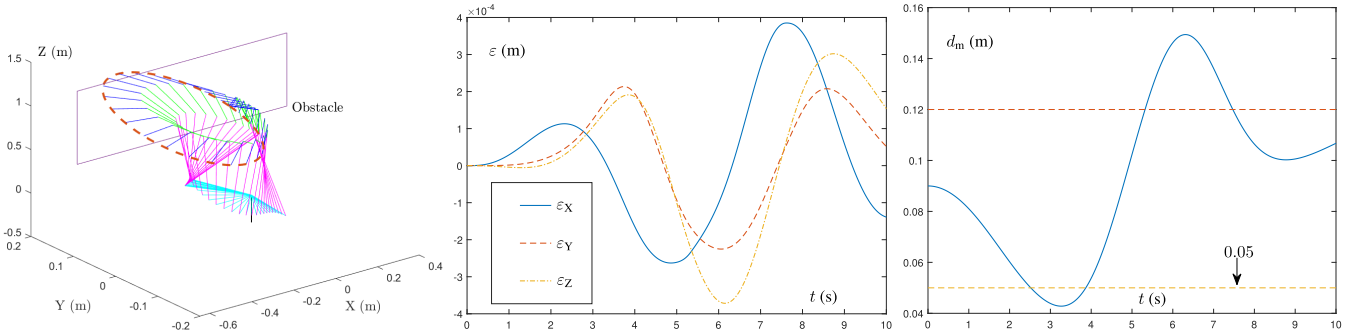

(a) Simulated path planning (b) End-effector planning error (c) Minimum link-obstacle distance

FIGURE 2. Simulation results of using the MAN scheme for the PA10 manipulator tracking the circular path in the presence of window-shaped obstacle.

computing the piecewise-linear equation as follows:

$$y - \mathcal{P}_{\Omega}(y - (Wy + q)) = 0, \tag{18}$$

where $y = [x^{\mathrm{T}}, \mu^{\mathrm{T}}, \nu^{\mathrm{T}}]^{\mathrm{T}} \in R^{n+m+\varrho}$ with $\mu \in R^{m}$ and $\nu \in R^{\varrho}$ denoting respectively the dual decision vectors of (15) and (16). Moreover, $\mathcal{P}_{\Omega}(\cdot)$ denotes the projection operator, and $W \in R^{(n+m+\varrho)\times(n+m+\varrho)}$ and $q \in R^{n+m+\varrho}$ are given by

$$W = \begin{bmatrix} Q & -J^{\mathrm{T}} & A^{\mathrm{T}} \\ J & 0 & 0 \\ -A & 0 & 0 \end{bmatrix}, \quad q = \begin{bmatrix} p \\ d \\ b. \end{bmatrix}$$

In this study, the following numerical algorithm [27] is used to compute (18) for determining the solution of (14)–(17):

$$\begin{cases} y^{k+1} = \mathcal{P}_{\Omega}\big(y^{k} - \rho(y^{k})\phi(y^{k})\big), \\ \rho(y^{k}) = \|e(y^{k})\|_2^2 / \|(W^{\mathrm{T}} + I)e(y^{k})\|_2^2, \\ \phi(y^{k}) = W^{\mathrm{T}} e(y^{k}) + Wy^{k} + q, \end{cases} \tag{19}$$

where the computing error $e(y^{k})$ is obtained by $e(y^{k}) = y^{k} - \mathcal{P}_{\Omega}(y^{k} - (Wy^{k} + q))$.

Taken together, the block diagram of the acceleration-level path-planning system for redundant manipulators, which incorporates the proposed ALOA scheme (7)–(12) and the numerical algorithm (19), is presented in Fig. 1.

IV. SIMULATION COMPARISON AND VALIDATION

In this section, under the PA10 manipulator with different obstacles (i.e., window-shaped and point obstacles), comparative simulation results are presented to validate the effective performance of the proposed ALOA scheme (7)–(12). In the simulations, the PA10 manipulator is equipped with a tool [23], and its initial state is set as $\theta(0) = [0, -\pi/4, 0, \pi/2, 0, -\pi/4, 0, -\pi/4]^{\mathrm{T}}$ rad. In addition, only the PA10 end-effector position is considered in the simulations. Table 1 presents the joint-physical limits of this manipulator, and the coefficients involved in (13) are set as $\vartheta = 0.1$ and $\kappa_{\mathrm{p}} = \kappa_{\mathrm{v}} = 25$. The feedback gains involved in (8) are set as $\alpha = \beta = 1.75$. Besides, in accordance with [27], the inner and outer thresholds for safety are set as 0.05 m and 0.12 m, respectively.

A. WINDOW-SHAPED OBSTACLE AVOIDANCE

In this subsection, with the window-shaped obstacle, we simulate the proposed ALOA scheme (7)–(12) for the PA10 manipulator to track the circular and tricuspid paths. The obstacle is given by four vertices at (0.35, 0.09, 1.42) m, (0.35, 0.09, 0.58) m, (−0.65, 0.09, 0.58) m, and (−0.65, 0.09, 1.42) m in the 3-D space. For comparison, the minimum acceleration norm (MAN) scheme is simulated, which is obtained by the proposed scheme without incorporating the inequality and bound constraints (9)–(12).

1) CIRCULAR PATH PLANNING EXAMPLE

By simulating the MAN scheme, Fig. 2 presents the related results, where the end-effector planning error is computed by $\varepsilon = \varphi(\theta) - r_{\mathrm{d}} \in R^{3}$. As presented in Fig. 2(a) and (b), the PA10 end-effector effectively moves along the desired circular path, where the maximal planning error is about 3.851×10^{-4} m. However, as presented in Fig. 2(c), at the initial time instant, the minimal link-obstacle distance denoted as d_{m} is larger than 0.05 m but smaller than 0.12 m. Such phenomenon indicates that the obstacle affects the PA10 manipulator. Moreover, as time evolves, the value of d_{m} decreases, and is less than 0.05 m during time $t \in [2.52, 3.84]$ s. This close distance (i.e., $d_{\mathrm{m}} < 0.05$ m) denotes that a collision exists [27], [28] and may damage the PA10 manipulator. These simulation results indicate that the MAN scheme cannot achieve the obstacle avoidance. Thus, an effective scheme, e.g., the proposed scheme (7)–(12), is worth developing and applying to the PA10 manipulator.

By simulating the proposed ALOA scheme (7)–(12), Fig. 3 presents the corresponding results. As presented in Fig. 3(a) and (b), the PA10 end-effector trajectory and the desired path are close to each other, with their maximal error being about 3.814×10^{-4} m. In addition, during the PA10 path planning, the value of d_{m} is always larger than 0.05 m, as presented in Fig. 3(c). This is because the inequality constraint (9) in the proposed scheme is activated when the obstacle is detected and is considered to be effective in the crucial region (i.e., $d_{\mathrm{m}} < 0.12$ m) [27], [28]. It follows from the appendix that (9) can generate an additional acceleration and the corresponding velocity. Such acceleration/velocity can make the PA10 joint configuration change accordingly.

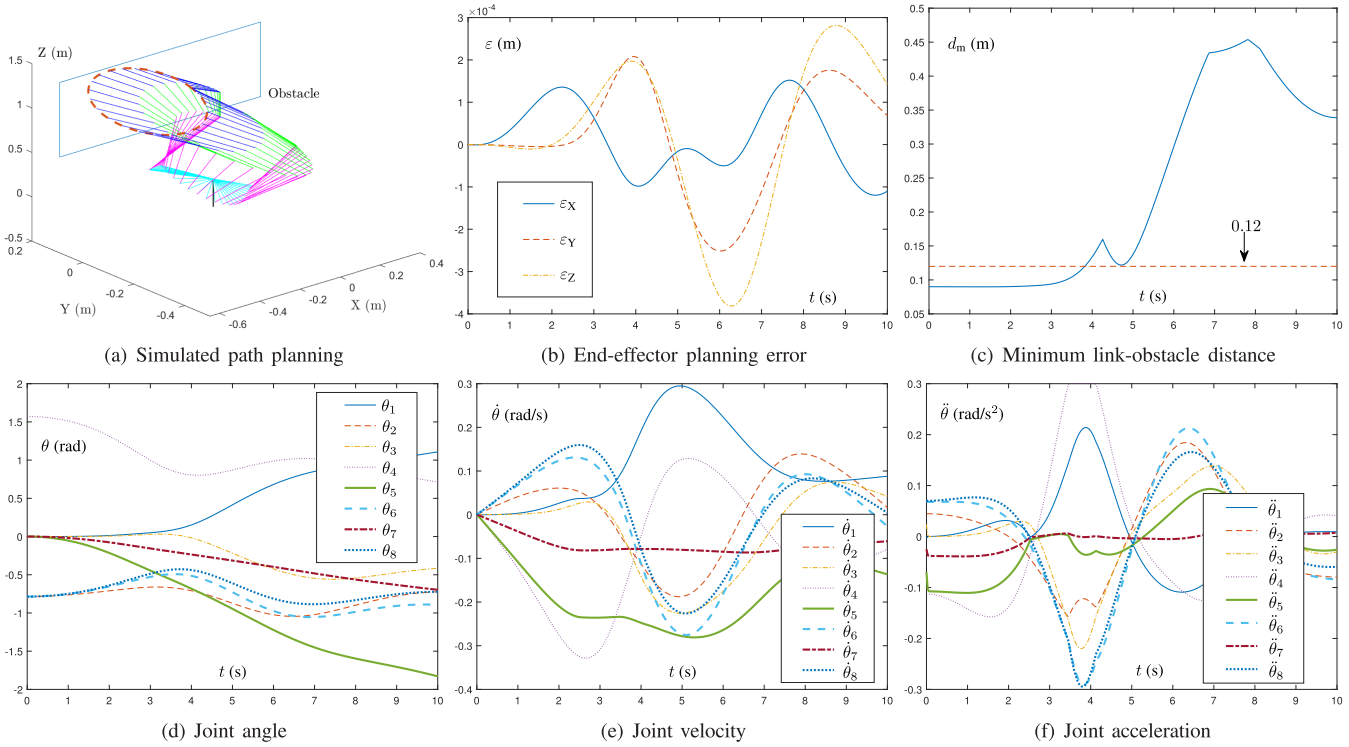

(a) Simulated path planning (b) End-effector planning error (c) Minimum link-obstacle distance

(d) Joint angle (e) Joint velocity (f) Joint acceleration

FIGURE 3. Simulation results of using the proposed ALOA scheme (7)–(12) for the PA10 manipulator tracking the circular path in the presence of window-shaped obstacle.

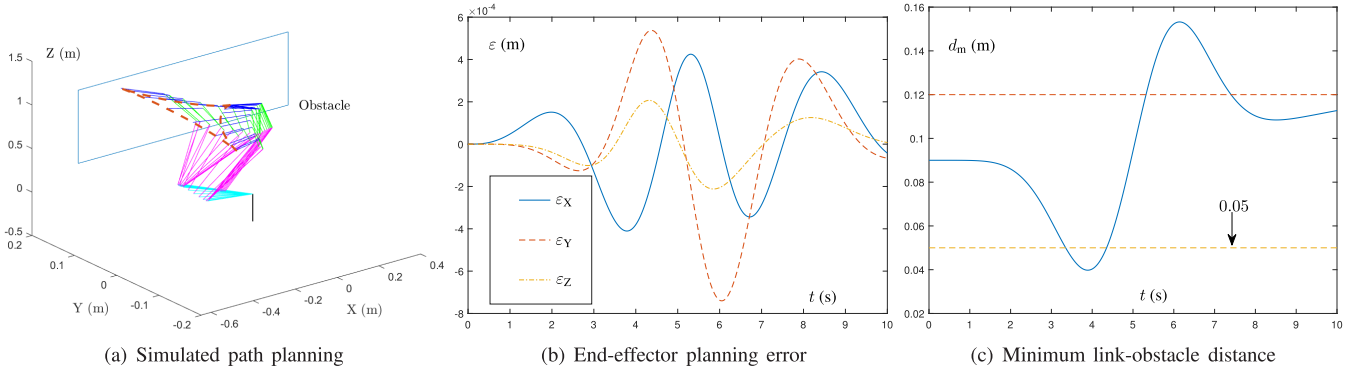

(a) Simulated path planning (b) End-effector planning error (c) Minimum link-obstacle distance

FIGURE 4. Simulation results of using the MAN scheme for the PA10 manipulator tracking the tricuspid path in the presence of window-shaped obstacle.

As time evolves, the value of d_{m} increases, and eventually is larger than 0.12 m. This phenomenon denotes that the PA10 manipulator has been away from the obstacle. In another words, the proposed ALOA scheme (7)–(12) effectively enables the obstacle avoidance of the PA10 manipulator. Besides, the solutions of θ and $\dot{\theta}$ presented in Fig. 3(d) and (e) are smooth and have not undergone abrupt changes. This phenomenon shows that the proposed acceleration-level scheme does not encounter the discontinuity issue of $\dot{\theta}$ that may arise in the velocity-level scheme [25], [27]. Furthermore, in Fig. 3(f), the solution of $\ddot{\theta}_4$ reaches (but does not exceed) its upper limit, and the solutions of $\ddot{\theta}_6$ and $\ddot{\theta}_8$ nearly reach their lower limits. In summary, because of the consideration and handle of physical limits for the PA10 manipulator, all the θ, $\dot{\theta}$, and $\ddot{\theta}$ solutions computed by (7)–(12) maintain within their limits. Evidently, the simulation results in Fig. 3 validate the effective performance of the proposed ALOA scheme (7)–(12).

2) TRICUSPID PATH PLANNING EXAMPLE

By simulating the MAN scheme, Fig. 4 presents the related results. In Fig. 4, although the PA10 end-effector effectively moves along the desired tricuspid path with a small planning error (i.e., in the order of 10^{-4} m), the minimal link-obstacle distance d_{m} is smaller than 0.05 m during time $t \in [3.35, 4.36]$ s. This statement means that the collision

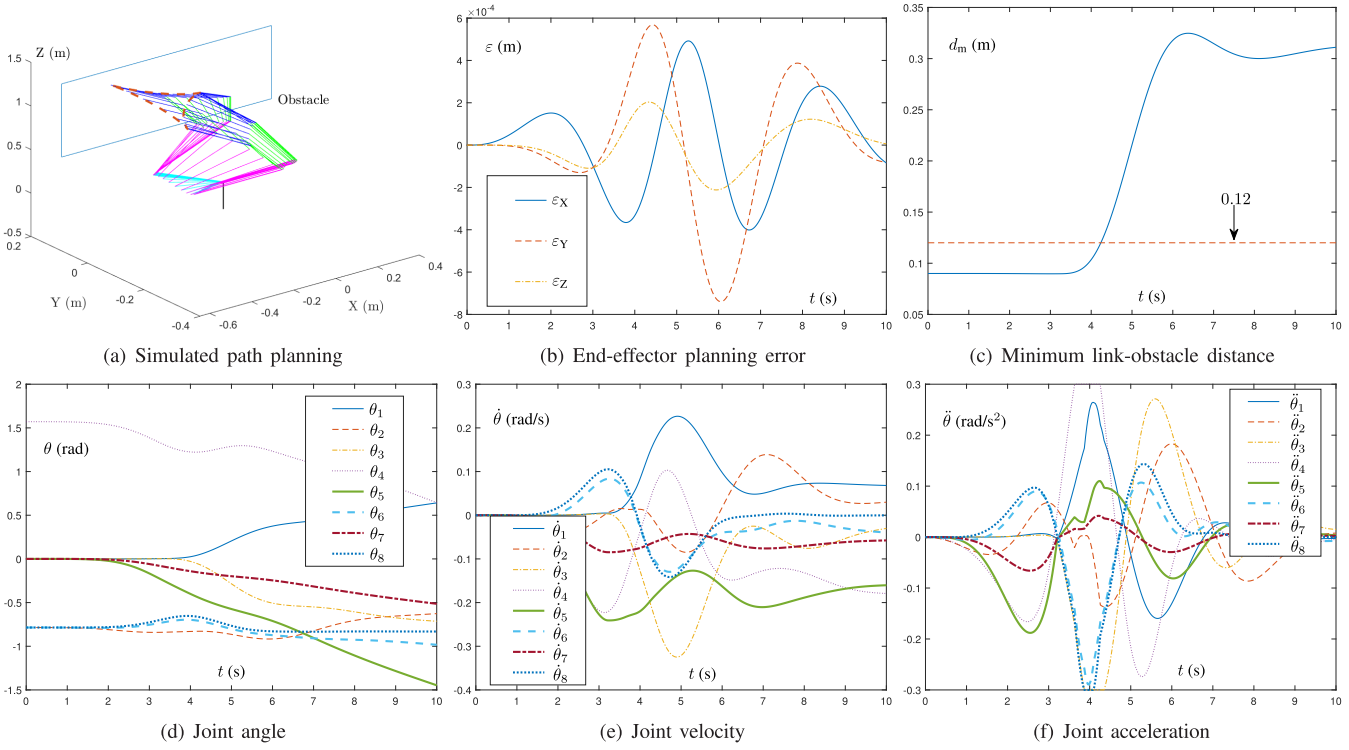

(a) Simulated path planning (b) End-effector planning error (c) Minimum link-obstacle distance

(d) Joint angle (e) Joint velocity (f) Joint acceleration

FIGURE 5. Simulation results of using the proposed ALOA scheme (7)–(12) for the PA10 manipulator tracking the tricuspid path in the presence of window-shaped obstacle.

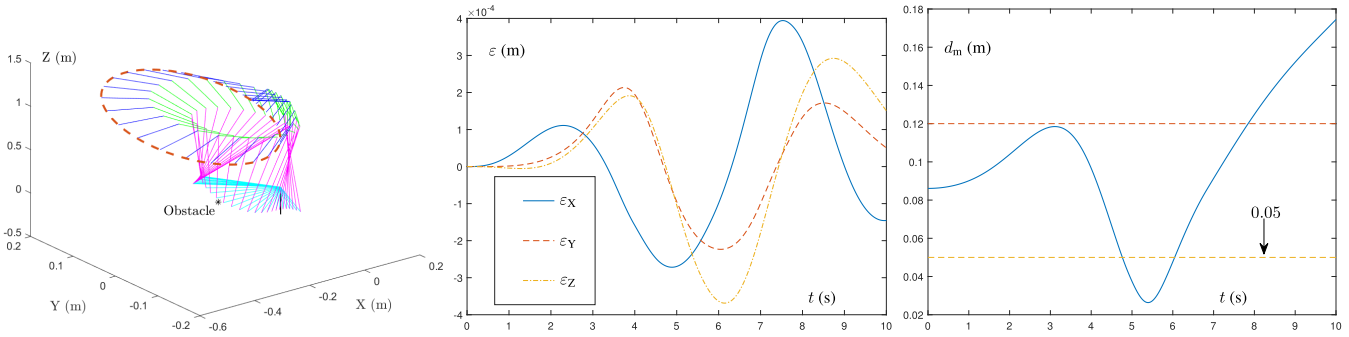

(a) Simulated path planning (b) End-effector planning error (c) Minimum link-obstacle distance

FIGURE 6. Simulation results of using the MAN scheme for the PA10 manipulator tracking the circular path in the presence of point obstacle.

exists in the tricuspid path planning of the PA10 manipulator. By contrast, Fig. 5 presents the corresponding results by simulating the proposed ALOA scheme (7)–(12). In Fig. 5(a)–(c), during the path planing execution, the value of d_{m} is always larger than 0.05 m, thereby indicating that (7)–(12) effectively enables the PA10 manipulator to avoid the obstacle. In Fig. 5(d)–(f), the θ and $\dot{\theta}$ solutions are smooth without abrupt change, and there does not exist the $\dot{\theta}$ discontinuity issue. Moreover, all the θ, $\dot{\theta}$, and $\ddot{\theta}$ solutions computed by (7)–(12) are kept within their limits, though the solutions of some joint accelerations reach the limits. In summary, these (comparative) simulation results verify that the proposed ALOA scheme (7)–(12) is effective in achieving the obstacle avoidance of the PA10 manipulator.

B. POINT OBSTACLE AVOIDANCE

In this subsection, we simulate the proposed ALOA scheme (7)–(12) for the PA10 manipulator to track three different paths (i.e., the circular, tricuspid, and Rhodonea paths) in the presence of point obstacle, where the obstacle point is at $(-0.35, -0.08, 0.32)$ m in the 3-D space.

By simulating the MAN scheme, Fig. 6 presents the related results, where the expected PA10 end-effector path is the circle. As presented in Fig. 6(a) and (b), the PA10 manipulator effectively conducts the circular path planning task, where the maximal end-effector planning error is about 3.942×10^{-4} m. However, as presented in Fig. 6(c), the minimal link-obstacle distance d_{m} is smaller than 0.05 m during time $t \in [4.77, 6.03]$ s, which means that the collision between the PA10 manipulator and point obstacle exists.

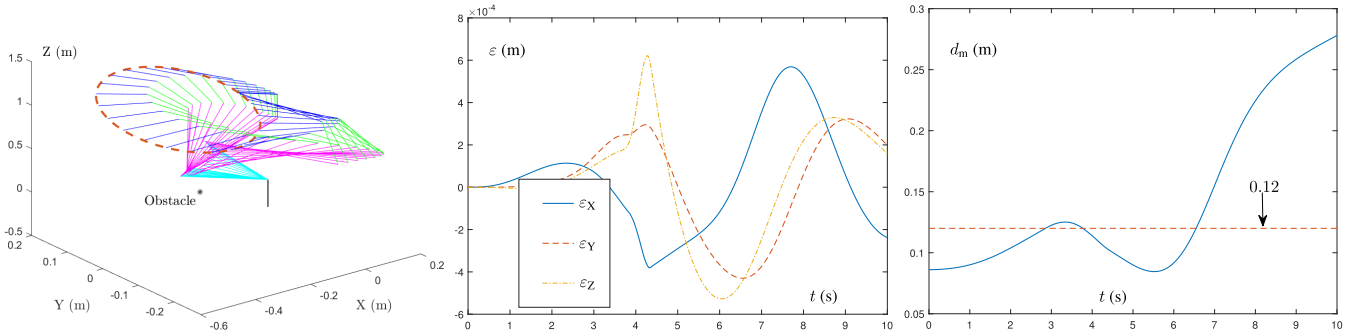

(a) Simulated path planning (b) End-effector planning error (c) Minimum link-obstacle distance

FIGURE 7. Simulation results of using the proposed ALOA scheme (7)–(12) for the PA10 manipulator tracking the circular path in the presence of point obstacle.

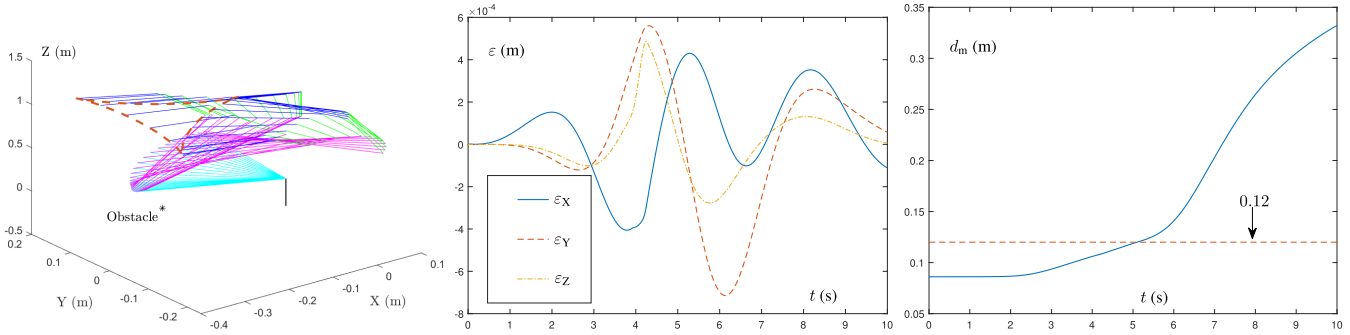

(a) Simulated path planning (b) End-effector planning error (c) Minimum link-obstacle distance

FIGURE 8. Simulation results of using the proposed ALOA scheme (7)–(12) for the PA10 manipulator tracking the tricuspid path in the presence of point obstacle.

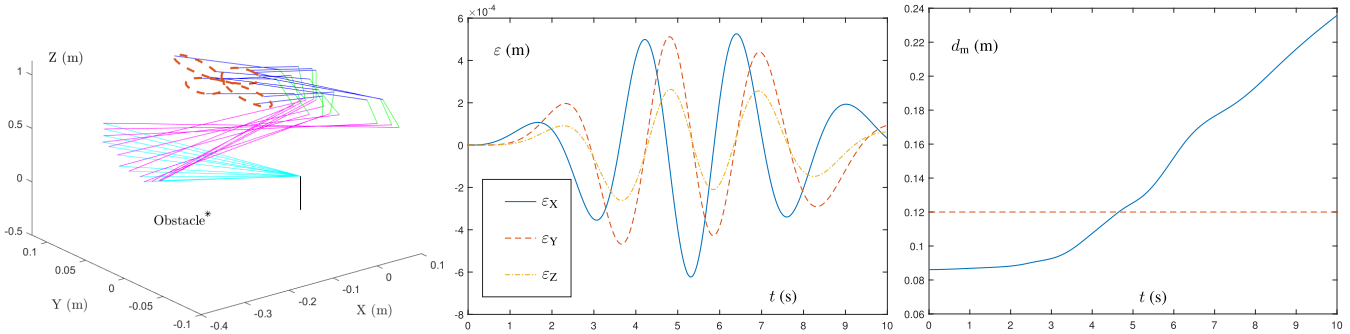

(a) Simulated path planning (b) End-effector planning error (c) Minimum link-obstacle distance

FIGURE 9. Simulation results of using the proposed ALOA scheme (7)–(12) for the PA10 manipulator tracking the Rhodonea path in the presence of point obstacle.

Therefore, the MAN scheme is ineffective in the obstacle avoidance despite enabling the PA10 end-effector path tracking.

To realize the avoidance of point obstacle, the proposed ALOA scheme (7)–(12) is simulated for the PA10 manipulator, and Fig. 7 presents the corresponding results. Evidently, Fig. 7 shows that the circular path planning task is successfully finished by the PA10 manipulator, with the maximal end-effector planning error being about 6.210×10^{-4} m. Moreover, because of activating the inequality constraint (9), the value of d_{m} is always larger than 0.05 m, thereby indicating that the point obstacle is effectively avoided for the PA10 manipulator using (7)–(12). Notably, the related results, which are omitted here owing to similarity, present that the proposed scheme does not encounter the discontinuity issue in the $\dot{\theta}$ solution, and maintains the solutions of θ, $\dot{\theta}$, and $\ddot{\theta}$ within their limits with smooth characteristics. These results validate the effective performance of the proposed ALOA scheme (7)–(12).

For further investigation, Figs. 8 and 9 present the results by simulating the proposed ALOA scheme (7)–(12), where the expected PA10 end-effector paths are the tricuspid and Rhodonea paths. As presented in such two figures, the PA10 manipulator effectively completes the desired

path planning task with a small end-effector planning error (i.e., in the order of 10^{-4} m), and the value of d_{m}, during the path planning execution, increases as time evolves, and eventually is larger than 0.12 m. Thus, the point obstacle avoidance is successfully realized for the PA10 manipulator using (7)–(12).

In summary, the aforementioned simulation results verify that the proposed ALOA scheme (7)–(12) effectively enables redundant manipulators to avoid obstacle at acceleration level.

V. CONCLUSION

In this study, the new acceleration-level inequality (4) that is capable of avoiding obstacle is designed and formulated. By combining the end-effector planning requirement and incorporating the joint-physical limits, the ALOA scheme (7)–(12) is proposed and investigated for redundant manipulators. Such scheme is transformed into the QP (14)–(17) and is computed by the numerical algorithm (19). Simulation results under the PA10 manipulator with window-shaped and point obstacles further validate the effective performance of the proposed ALOA scheme (7)–(12).

One future research direction can be the study of (7)–(12) for redundant manipulators with joint-torque limits considered. Another is the design of a new obstacle avoidance scheme with noise tolerance property for redundant manipulators [15], [30].

ACKNOWLEDGMENT

The authors thank the editors and reviewers for the time and effort spent in reviewing this article and the suggestions provided to further improve its presentation and quality.

APPENDIX

In this appendix, the derivation of the new acceleration-level inequality (4) for obstacle avoidance is presented.

Specifically, to realize the avoidance of obstacle for redundant manipulators, an additional acceleration $\ddot{r}_C$ is used, which has a variable magnitude $\xi = [\xi_{\mathrm{X}}, \xi_{\mathrm{Y}}, \xi_{\mathrm{Z}}]^{\mathrm{T}}$ with $\xi_{\mathrm{X}} \geqslant 0$, $\xi_{\mathrm{Y}} \geqslant 0$, and $\xi_{\mathrm{Z}} \geqslant 0$. This additional acceleration is assigned at point C to make the manipulator leave obstacle. Mathematically,

$$J_C\ddot{\theta} + \dot{J}_C\dot{\theta} = \ddot{r}_C = \begin{bmatrix} \xi_{\mathrm{X}}(x_C - x_O) \\ \xi_{\mathrm{Y}}(y_C - y_O) \\ \xi_{\mathrm{Z}}(z_C - z_O) \end{bmatrix}, \tag{20}$$

where J_C, $\dot{J}_C$, (x_C, y_C, z_C), and (x_O, y_O, z_O) are defined the same as those in Section II-B.

Let us recall the definition of $\overrightarrow{r}$, i.e., $\overrightarrow{r} = [x_C - x_O, y_C - y_O, z_C - z_O]$. Left multiplying $-\overrightarrow{r}$ in (20) yields

$$\begin{aligned} -\overrightarrow{r}(J_C\ddot{\theta} + \dot{J}_C\dot{\theta}) &= -\overrightarrow{r}\begin{bmatrix} \xi_{\mathrm{X}}(x_C - x_O) \\ \xi_{\mathrm{Y}}(y_C - y_O) \\ \xi_{\mathrm{Z}}(z_C - z_O) \end{bmatrix} \\ &= -\xi_{\mathrm{X}}(x_C - x_O)^2 - \xi_{\mathrm{Y}}(y_C - y_O)^2 \\ &\quad -\xi_{\mathrm{Z}}(z_C - z_O)^2. \end{aligned}$$

Because of ξ_{X}, ξ_{Y}, and ξ_{Z} being nonnegative, the following result is further obtained:

$$-\overrightarrow{r}(J_C\ddot{\theta} + \dot{J}_C\dot{\theta}) \leqslant 0,$$

which is rewritten as

$$-\overrightarrow{r}J_C\ddot{\theta} \leqslant \overrightarrow{r}\dot{J}_C\dot{\theta}. \tag{21}$$

By defining $A = -\overrightarrow{r}J_C$ and $B = \overrightarrow{r}\dot{J}_C$, (21) becomes

$$A\ddot{\theta} \leqslant B\dot{\theta},$$

which is exactly the new acceleration-level inequality (4) that is designed in this study for realizing the obstacle avoidance at acceleration level.

Thus, on the basis of the above derivation, the inequality (4) can generate the additional acceleration with variable magnitude and the related velocity to enable redundant manipulators to avoid the obstacle at acceleration level.

REFERENCES

[1] B. Siciliano, L. Sciavicco, L. Villani, and G. Oriolo, *Robotics: Modeling, Planning and Control*. London, U.K.: Springer-Verlag, 2009.
[2] Y. Zhang and L. Jin, *Robot Manipulator Redundancy Resolution*. Hoboken, NJ, USA: Wiley, 2017.
[3] L. Jin, S. Li, J. Yu, and J. He, "Robot manipulator control using neural networks: A survey," *Neurocomputing*, vol. 285, pp. 23–34, Apr. 2018.
[4] Y. Zhang, S. Chen, S. Li, and Z. Zhang, "Adaptive projection neural network for kinematic control of redundant manipulators with unknown physical parameters," *IEEE Trans. Ind. Electron.*, vol. 65, no. 6, pp. 4909–4920, Jun. 2017.
[5] S. Li, L. Jin, and M. A. Mirza, *Kinematic Control of Redundant Robot Arms Using Neural Networks*. Hoboken, NJ, USA: Wiley, 2019.
[6] J. Kim and E. A. Croft, "Online near time-optimal trajectory planning for industrial robots," *Robot. Comput. Integr. Manuf.*, vol. 58, pp. 158–171, 2019.
[7] V. V. M. J. S. Chembuly and H. K. Voruganti, "Trajectory planning of redundant manipulators moving along constrained path and avoiding obstacles," *Procedia Comput. Sci.*, vol. 133, pp. 627–634, 2018.
[8] D. Han, H. Nie, J. Chen, and M. Chen, "Dynamic obstacle avoidance for manipulators using distance calculation and discrete detection," *Robot. Comput.-Integr. Manuf.*, vol. 49, pp. 98–104, Feb. 2018.
[9] A. Jiang, X. Yao, and J. Zhou, "Research on path planning of real-time obstacle avoidance of mechanical arm based on genetic algorithm," *J. Eng.*, vol. 2018, no. 16, pp. 1579–1586, 2018.
[10] N. Rahmanian-Shahri and I. Troch, "Collision-avoidance for redundant robots through control of the self-motion of the manipulator," *J. Intell. Robot. Syst.*, vol. 16, no. 2, pp. 123–149, 1996.
[11] K.-K. Lee and M. Buss, "Obstacle avoidance for redundant robots using Jacobian transpose method," in *Proc. IEEE/RSJ Int. Conf. Intell. Robots Syst.*, Oct. 2007, pp. 3509–3514.
[12] F. Padula and V. Perdereau, "A new pseudoinverse for manipulator collision avoidance," *IFAC Proc.*, vol. 44, no. 1, pp. 14687–14692, 2011.
[13] M. G. Marcos, J. A. T. Machado, and T.-P. Azevedo-Perdicoúlis, "A multi-objective approach for the motion planning of redundant manipulators," *Appl. Soft Comput.*, vol. 12, no. 2, pp. 589–599, 2012.
[14] X. Wang, C. Yang, J. Chen, H. Ma, and F. Liu, "Obstacle avoidance for kinematically redundant robot," *IFAC-PapersOnLine*, vol. 48, no. 28, pp. 490–495, 2015.
[15] D. Guo, F. Xu, L. Yan, Z. Nie, and H. Shao, "A new noise-tolerant obstacle avoidance scheme for motion planning of redundant robot manipulators," *Frontiers Neurorobot.*, vol. 12, pp. 51–63, Aug. 2018.
[16] O. Khatib, "Real-time obstacle avoidance for manipulators and mobile robots," *Int. J. Robot. Res.*, vol. 5, no. 1, 90–98, 1986.
[17] R. Volpe and P. Khosla, "Manipulator control with superquadric artificial potential functions: Theory and experiments," *IEEE Trans. Syst., Man, Cybern.*, vol. 20, no. 6, pp. 1423–1436, Nov./Dec. 1990.

[18] T. Tsuji, Y. Tanaka, P. G. Morasso, V. Sanguineti, and M. Kaneko, "Bio-mimetic trajectory generation of robots via artificial potential field with time base generator," *IEEE Trans. Syst., Man, C, Appl. Rev.*, vol. 32, no. 4, pp. 426–439, Nov. 2002.
[19] L. M. Capisani and A. Ferrara, "Trajectory planning and second-order sliding mode motion/interaction control for robot manipulators in unknown environments," *IEEE Trans. Ind. Electron.*, vol. 59, no. 8, pp. 3189–3198, Aug. 2012.
[20] U. Orozco-Rosas, O. Montiel, and R. Sepúlveda, "Mobile robot path planning using membrane evolutionary artificial potential field," *Appl. Soft Comput. J.*, vol. 77, pp. 236–251, Apr. 2019.
[21] F.-T. Cheng, T.-H. Chen, Y.-S. Wang, and Y.-Y. Sun, "Obstacle avoidance for redundant manipulators using the compact QP method," in *Proc. IEEE Int. Conf. Robot. Autom.*, vol. 3, May 1993, pp. 262–269.
[22] W. Tang, L. Lam, and J. Wang, "Kinematic control and obstacle avoidance for redundant manipulators using a recurrent neural network," in *Proc. Int. Conf. Artif. Neural Netw.*, 2001, pp. 922–929.
[23] Y. Zhang and J. Wang, "Obstacle avoidance for kinematically redundant manipulators using a dual neural network," *IEEE Trans. Syst., Man, Cybern. B, Cybern.*, vol. 34, no. 1, pp. 752–759, Feb. 2004.
[24] X. Hu, J. Wang, and B. Zhang, "Motion planning with obstacle avoidance for kinematically redundant manipulators based on two recurrent neural networks," in *Proc. Int. Conf. Syst., Man, Cybern.*, 2009, pp. 137–142.
[25] D. Guo and Y. Zhang, "A new inequality-based obstacle-avoidance mvn scheme and its application to redundant robot manipulators," *IEEE Trans. Syst., Man, Cybern. C, Appl. Rev.*, vol. 42, no. 6, pp. 1326–1340, Jun. 2012.
[26] D. Chen and Y. Zhang, "A hybrid multi-objective scheme applied to redundant robot manipulators," *IEEE Trans. Autom. Sci. Eng.*, vol. 14, no. 3, pp. 1337–1350, Jul. 2017.
[27] D. Guo and Y. Zhang, "Acceleration-level inequality-based man scheme for obstacle avoidance of redundant robot manipulators," *IEEE Trans. Ind. Electron.*, vol. 61, no. 12, pp. 6903–6914, Dec. 2014.
[28] D. Guo and K. Li, "Acceleration-level obstacle-avoidance scheme for motion planning of redundant robot manipulators," in *Proc. IEEE Int. Conf. Robot. Biomim.*, Dec. 2016, pp. 1313–1318.
[29] L. Xiao and Y. Zhang, "Dynamic design, numerical solution and effective verification of acceleration-level obstacle avoidance scheme for robot manipulators," *Int. J. Syst. Sci.*, vol. 47, no. 4, pp. 932–945, 2016.
[30] Z. Li, B. Liao, F. Xu, and D. Guo, "A new repetitive motion planning scheme with noise suppression capability for redundant robot manipulators," *IEEE Trans. Syst., Man, Cybern., Syst.*, to be published.
[31] D. Guo, K. Li, and B. Liao, "Bi-criteria minimization with MWVN-INAM type for motion planning and control of redundant robot manipulators," *Robotica*, vol. 36, no. 5, pp. 655–675, 2018.
[32] R. M. Murray, Z. Li, and S. S. Sastry, *A Mathematical Introduction to Robotic Manipulation*. Boca Raton, FL, USA: CRC Press, 1994.
[33] Y. Zhang, D. Guo, and S. Ma, "Different-level simultaneous minimization of joint-velocity and joint-torque for redundant robot manipulators," *J. Intell. Robot. Syst.*, vol. 72, nos. 3–4, pp. 301–323, 2013.

DONGSHENG GUO (S'12–M'16) received the B.S. degree in automation from Sun Yat-sen University, Guangzhou, China, in 2010, and the Ph.D. degree in communication and information systems from the School of Information Science and Technology, Sun Yat-sen University, in 2015. He is currently an Associate Professor with the College of Information Science and Engineering, Huaqiao University, Xiamen, China, and with the Fujian Engineering Research Center of Motor Control and System Optimal Schedule, Xiamen, for cooperative research. His current research interests include robotics, neural networks, and numerical methods.

QINGSHAN FENG received the B.S. degree in automation from Huaqiao University, Xiamen, China, in 2018, where he is currently pursuing the M.S. degree in control science and engineering with the College of Information Science and Engineering. His current research interests include robotics and numerical methods.

JIANHUANG CAI received the B.S. degree in automation from Huaqiao University, Xiamen, China, in 2018, where he is currently pursuing the M.S. degree in control science and engineering with the College of Information Science and Engineering. His current research interests include neural networks and optimization.